Coordinated Standoff Tracking of Moving Target Groups Using Multiple UAVs

HYONDONG OH
Loughborough University
Loughborough, United Kingdom

SEUNGKEUN KIM
Chungnam National University
Daejeon, Republic of Korea

HYO-SANG SHIN
ANTONIOS TSOURDOS
Cranfield University
Cranfield, United Kingdom

This paper presents a methodology for coordinated standoff tracking of moving target groups using multiple unmanned aerial vehicles (UAVs). The vector field guidance approach for a single UAV is first applied to track a group of targets by defining a variable standoff orbit to be followed, which can keep all targets within the field-of-view of the UAV. A new feedforward term is included in the guidance command considering variable standoff distance, and the convergence of the vector field to the standoff orbit is analyzed and enhanced by adjusting radial velocity using two active measures associated with vector field generation. Moreover, for multiple group tracking by multiple UAVs, a two-phase approach is proposed as a suboptimal solution for a Non-deterministic Polynomial-time hard (NP-hard) problem, consisting of target clustering/assignment and cooperative standoff group tracking with online local replanning. Lastly, localization sensitivity to the group of targets is investigated for different angular separations between UAVs and sensing configurations. Numerical simulations are performed using randomly moving ground vehicles with multiple UAVs to verify the feasibility and benefit of the proposed approach.

Manuscript received January 16, 2014; revised August 30, 2014; released for publication November 13, 2014.

DOI. No. 10.1109/TAES.2015.140044.

Refereeing of this contribution was handled by L. Rodrigues.

This study was supported by 1) the UK Engineering and Physical Science Research Council (EPSRC) under Grant EP/J011525/1 and 2) a grant to Bio-Mimetic Robot Research Center funded by Defense Acquisition Program Administration (UD130070ID).

Authors' address: H. Oh, Department of Aeronautical and Automotive Engineering, Loughborough University, Loughborough, Leicestershire, LE11 3TU, United Kingdom; S. Kim, Department of Aerospace Engineering, Chungnam National University, 99 Daehak-ro, Yuseong-gu, Daejeon 305-764, Republic of Korea, E-mail: (skim78@cnu.ac.kr); H.-S. Shin and A. Tsourdos, Division of Engineering Sciences, Cranfield University, Cranfield, MK43 0AL, United Kingdom.

0018-9251/15/$26.00 © 2015 IEEE

I. INTRODUCTION

In recent decades, unmanned aerial vehicle (UAV) team operations have received increasing attention in both military and civil sectors owing to their cooperation and coordination capabilities to achieve common goals with simultaneous coverage of large areas. Searching and subsequent tracking of moving ground targets of interest are primary capabilities of UAVs required to predict the target's intent and to take proactive measures. Specific applications under consideration are border patrol [1, 2], airborne surveillance [3, 4], and police law enforcement [5, 6].

In performing such missions, due to the possible speed superiority over the ground targets, fixed-wing UAVs require a certain motion planning or guidance algorithm to persistently track the target in consideration of their operational and physical constraints. For this, a circular standoff line-of-sight (LOS) tracking concept is introduced to closely orbit around the target while maintaining sensor coverage and remaining outside a critical threat range. In [7–9], vector field-based approaches were proposed to guide the UAV to a stable vector field around a target. Zhu et al. [10, 11] proposed a similar approach considering input constraints explicitly. Shames et al. [12, 13] addressed a tracking problem (termed as target localization and circumnavigation) making the UAV loiter around a target such that both the target estimator and the control systems remained stable. An optimal path planning approach was also proposed to provide convoy overwatch for a moving ground vehicle in [14]. Wise and Rysdyk [15] compared the different methodologies for circular LOS tracking. These circular flights are recommended for various target tracking applications, because for each UAV, the maximum altitude flight ensures the maximum visibility, and the minimum radius turn keeps the minimum distance to the target at the maximum altitude [16]. Standoff target tracking using cooperative UAVs is also proposed by distributing a team of UAVs on a standoff orbit when the target vehicle is uncooperative, or is highly agile [17–20]. This cooperative standoff tracking of a moving target using multiple UAVs can provide better estimation accuracy with sensor/data fusion through communication between UAVs [21, 22]. It is also shown to provide more robust tracking performance in cases where one of the UAVs has temporary sensing failure or LOS blockage by obstacles [16].

However, the aforementioned previous research on standoff tracking has focused only on the single target tracking problem. When multiple moving ground vehicles are identified as targets of interest from reconnaissance or surveillance systems within the ground road traffic [23, 24], strategies must be developed to address how to deploy multiple UAVs to persistently follow them. Although various different methodologies have been developed for multiple-target tracking using multiple ground [25, 26] or aerial vehicles [27–29], there is relatively little research on multiple or group target tracking in the context of

cooperative standoff LOS tracking subject to uncertain dynamic environments and UAV sensing capability. In particular, the existing works in [27] and [28] focus on a mission planning side (more specifically, visiting order determination and optimal path planning) with perfectly known target positions and without much consideration on sensing constraints. Meanwhile, this paper introduces an online guidance and estimation algorithm to guarantee tracking of all targets within the field-of-view (FOV) of the sensor at all times for persistent tracking and surveillance purposes. As multiple UAVs are always overseeing targets within a sensor range, they can easily and quickly cope with environment/situation changes with continuous guidance commands. Although similar work was done by Deghat et al. [29] for simultaneous localization and circular tracking of multiple targets, their approach was only for a single UAV tracking a fixed number of targets without any autonomous decision-making process.

Therefore, this paper proposes a methodology for coordinated standoff tracking of moving target groups using multiple UAVs. In order to track a group of targets using the sensor with a limited FOV, the vehicle should be positioned as close as possible to multiple targets to obtain better estimation accuracy and far enough to keep the group of targets within its FOV. For this, amongst many standoff tracking guidance algorithms, the vector field guidance approach is selected since it produces stable convergence to a circling limit cycle [7, 30]. The objective of this study is to develop an active sensing/guidance algorithm to maximize information or estimation accuracy of targets as well as persistently keep all of them (or as many as possible) within the view of multiple UAVs while considering physical (turning radius and speed) and sensing (FOV and range) constraints.

The main contributions of this paper are fourfold. First, this paper proposes a new coordinated group target tracking method in the context of standoff tracking by defining a variable standoff orbit to be followed. This proposed tracking method can keep all targets within the FOV of the UAV even under uncertainty of estimated target information. Second, a new feedforward term is computed in the guidance command considering variable standoff distance compared to a single target tracking case having constant standoff distance. Moreover, convergence of the vector field to the variable standoff orbit is analyzed and enhanced by adjusting radial velocity using two active measures associated with vector field generation. Third, for multiple group target surveillance by multiple UAVs, a two-phase approach is proposed as a suboptimal solution for a Non-deterministic Polynomial-time hard (NP-hard) problem: 1) Multiple targets are clustered using *K*-means clustering algorithm, and UAVs are assigned to the appropriate target group in a way that maximizes information defined by the Fisher information matrix (FIM), and then 2) cooperative standoff group tracking is performed with online local replanning, including target handoff and discard from the group according to sensing capability and vector field convergence. Last, localization

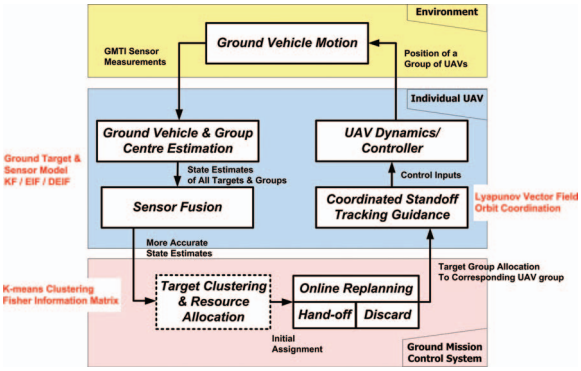

Fig. 1. Flow chart of overall algorithm for coordinated standoff tracking scheme.

sensitivity to the group of targets is investigated for different angular separations between UAVs and sensing configurations as a basis for a future optimal separation scheme. Fig. 1 shows a flow chart of the overall algorithm for the proposed coordinated standoff tracking scheme for multiple UAVs.

The overall structure of this paper is given as follows. Section II contains problem formulation, including assumptions made in this study and tracking filter design with a UAV kinematic, ground target, and sensor model. Section III proposes the standoff tracking guidance algorithm for a group of moving targets using a single UAV, followed by tracking of several groups of targets using multiple cooperating UAVs in section IV. Section V presents numerical simulation results of a group target tracking scenario. Last, conclusions and future work are given in section VI.

II. PROBLEM FORMULATION

It is first assumed that the lateral and longitudinal dynamics of the UAV can be decoupled as in conventional fixed-wing aircraft. Therefore, a two-dimensional space is considered for the UAV flying at a constant altitude. In this study, it is also assumed that initial target information is given by other sources such as a search-and-monitoring UAV [23], and an onboard sensor can point at the group center using a gimbal system. Note that data association for multiple targets and communications between UAVs are not the scope of this study. UAV team members share a known global coordinate system such as the global positioning system (GPS) for their own and the targets' position. The concept of the standoff tracking problem of moving target groups using multiple UAVs is illustrated in Fig. 2. The standoff orbit for each group followed by UAVs needs to be changed in terms of size and location according to the dispersion of the moving targets so that all targets can be inside the FOV of UAVs.

A. UAV Dynamic Model

Assuming each UAV has a low-level flight controller such as a stability augmentation system (SAS) and controllability augmentation system (CAS) for heading

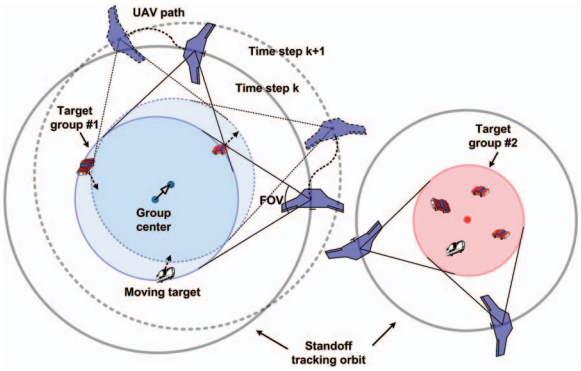

Fig. 2. Illustration of standoff tracking of moving target groups using multiple UAVs considering sensing constraints.

and velocity hold functions, this study aims to design guidance inputs to this low-level controller for standoff target tracking. Consider a two-dimensional UAV kinematic model [18] as:

$$\begin{pmatrix} \dot{x} \\ \dot{y} \\ \dot{\psi} \\ \dot{v} \\ \dot{\omega} \end{pmatrix} = f(\mathbf{x}, \mathbf{u}) = \begin{pmatrix} v\cos\psi \\ v\sin\psi \\ \omega \\ -\frac{1}{\tau_v}v + \frac{1}{\tau_v}u_v \\ -\frac{1}{\tau_\omega}\omega + \frac{1}{\tau_\omega}u_\omega \end{pmatrix} \tag{1}$$

where $\mathbf{x} = (x, y, \psi, v, \omega)^T$ are the inertial position, heading, speed, and yaw rate of the UAV, respectively; τ_v and τ_ω are time constants for considering actuator delay; and $\mathbf{u} = (u_v, u_\omega)^T$ are the commanded speed and turning rate constrained by the following dynamic limits of fixed-wing UAVs:

$$|u_v - v_0| \leq \Delta v_{max} \tag{2}$$

$$|u_\omega| \leq \omega_{max} \tag{3}$$

where v_0 is the nominal speed of the UAV. The continuous UAV model in (1) can be discretized by Euler integration into:

$$\mathbf{x}_{k+1} = f_d(\mathbf{x}_k, \mathbf{u}_k) = \mathbf{x}_k + T_s f(\mathbf{x}_k, \mathbf{u}_k) \tag{4}$$

where $\mathbf{x}_k = (x_k, y_k, \psi_k, v_k, \omega_k)^T$, $\mathbf{u}_k = (u_{vk}, u_{\omega k})^T$, and T_s is a sampling time.

B. Ground Target and Sensor Model

General target tracking filters have traditionally been developed for monitoring aerial targets such as airplanes, missiles, and so on. Although ground vehicles move with much lower speeds than aerial targets, they often perform irregular stop-and-go maneuvers with a much smaller turn radius. A constant-velocity model usually used for radar target tracking is thus unsuitable for tracking ground vehicles, and hence an acceleration or jerk model is a more suitable model. After analyzing the car trajectory data acquired by running the S-Paramics traffic simulation software [31] (Fig. 3a) and considering general driving behavior, it is observed that the jerk is not negligible, with

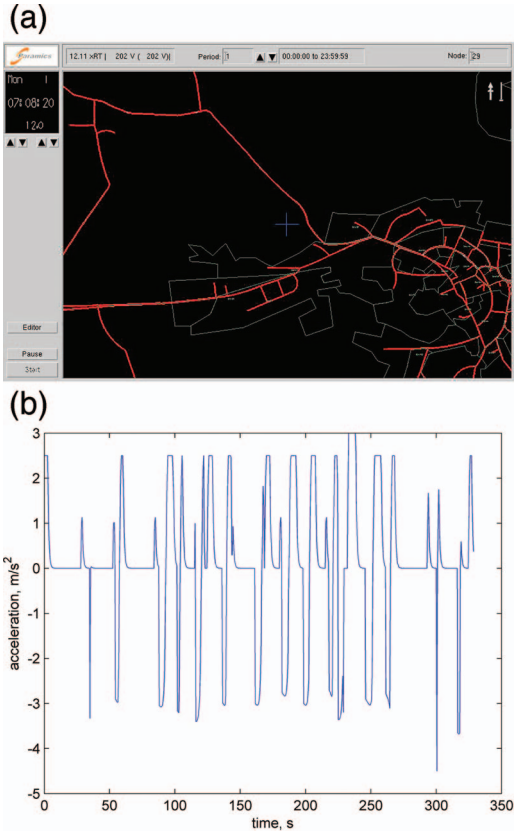

Fig. 3. S-Paramics traffic model of Devizes, Wiltshire, United Kingdom.

the acceleration best modeled using a piecewise constant profile over a specific duration of time, as shown in Fig. 3b. Hence, a good model to apply to the tracking of ground targets considers acceleration dynamics [32]. This acceleration model defines the target acceleration as a correlated process with a decaying exponential autocorrelation function, which means if there is a certain acceleration rate at a time t, then it is likely to be correlated via the exponential at a time instant t $+\tau$. A discretized system equation for the acceleration model for a ground vehicle is thus expressed in the form:

$$\mathbf{x}_{k+1}^t = F_k \mathbf{x}_k^t + \eta_k \tag{5}$$

where the state vector is $\mathbf{x}_k^t = (x_k^t, \dot{x}_k^t, \ddot{x}_k^t, y_k^t, \dot{y}_k^t, \ddot{y}_k^t)^T$, and where η_k is a process noise that represents the acceleration characteristics of the target. The state transition matrix F_k is given by [32]:

$$F_k = \begin{bmatrix} F_{1k} & \mathbf{0} \\ \mathbf{0} & F_{1k} \end{bmatrix} \tag{6}$$

where $F_{1k} = \begin{bmatrix} 1 & T_s & (e^{-\alpha T_s} + \alpha T_s - 1)/\alpha^2 \\ 0 & 1 & (1 - e^{-\alpha T_s})/\alpha \\ 0 & 0 & e^{-\alpha T_s} \end{bmatrix}$, and α is a correlation parameter that models different classes of targets: a small α for targets with relatively slow maneuvers and a high α for targets with fast and evasive

maneuvers. The details of acceleration dynamics can be found in [18].

In addition, this study assumes that UAVs are equipped with a ground moving target indicator (GMTI) sensor to localize the position of target. To produce appropriate surveillance data for multiple targets, a GMTI is a well-suited sensor due to its wide coverage and real-time capabilities [33]. Since the measurement of a GMTI is composed of range and azimuth of the target with respect to the radar location, the actual measurements are the relative range and azimuth with respect to the position of the UAV. The radar measurement $\mathbf{z}_k = (r_k, \theta_k)^T$ can be defined as the following nonlinear relation using the target position $(x_k^t, y_k^t)^T$ and the UAV position $(x_k, y_k)^T$ as:

$$\begin{pmatrix} r_k \\ \theta_k \end{pmatrix} = h(\mathbf{x}_k^t) + v_k = \begin{pmatrix} \sqrt{(x_k^t - x_k)^2 + (y_k^t - y_k)^2} \\ \tan^{-1}\frac{y_k^t - y_k}{x_k^t - x_k} \end{pmatrix} + v_k \tag{7}$$

where v_k is a measurement noise vector, and its noise covariance matrix is defined as: $V_n[v_k] = R_k = diag([\sigma_r^2, \sigma_\theta^2])$.

C. Ground Target Tracking Filter

Considering the nonlinear measurement equation as in (7) and the advantage of using information from multisensor systems, target localization is performed by using the extended information filter (EIF) [34] as:

Prediction

$$\mathbf{y}_{k|k-1}^t = Y_{k|k-1} F_k Y_{k-1|k-1}^{-1} \mathbf{y}_{k-1|k-1}^t \tag{8}$$

$$Y_{k|k-1} = \left(F_k Y_{k-1|k-1}^{-1} F_k^T + Q_k\right)^{-1} \tag{9}$$

Update

$$\mathbf{y}_{k|k}^t = \mathbf{y}_{k|k-1}^t + H_k^T (R_k)^{-1} \cdot [\mathbf{z}_k - h(\mathbf{x}_{k|k-1}^t) + H_k \mathbf{x}_{k|k-1}^t] \tag{10}$$

$$Y_{k|k} = Y_{k|k-1} + H_k^T (R_k)^{-1} H_k \tag{11}$$

where $Y_k = (P_k)^{-1}$ and $\mathbf{y}_k^t = Y_k \mathbf{x}_k^t$ represent the information matrix and information state vector, respectively. The output matrix H_k is a Jacobian of (7) with respect to the time-update state $\mathbf{x}_{k|k-1}^t$. Given that multiple UAVs carry out the coordinated standoff tracking of groups of targets, each UAV's GMTI sensor obtains its own measurement and executes the tracking filter algorithm separately. After each UAV receives the other's estimation via communications, a decentralized EIF is applied to enhance the tracking accuracy [34, 35]. It is worthwhile noting that the estimation performance can be further improved by converting range and bearing measurement to inertial measurements before they are incorporated into the Kalman filter as shown in [36]. Depending on the noise characteristics of the measurements, the linear Kalman filter (when the bearing measurement is known to be accurate), the extended Kalman filter (EKF), or the unscented Kalman filter could be used with corresponding conversion techniques [37, 38].

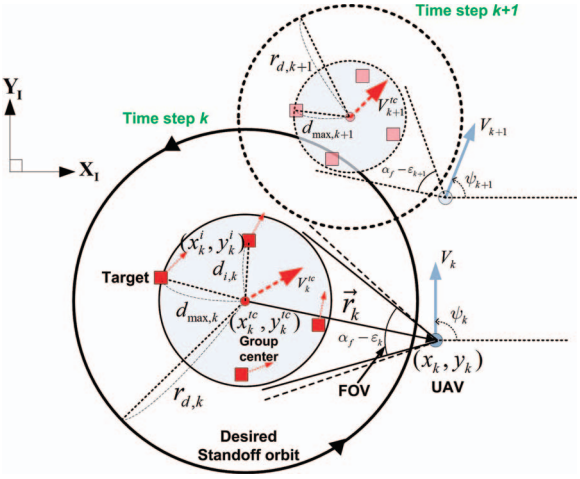

Fig. 4. Geometric relation among UAV, ground target, and target group at time step k and $k+1$.

Having estimated all available targets' information, the information on the center of a target group is also estimated using the same target model as in section IIB, position measurements of the geometric centroid for targets in the group, and a linear Kalman filter providing $\mathbf{x}_k^{tc} = (x_k^{tc}, \dot{x}_k^{tc}, \ddot{x}_k^{tc}, y_k^{tc}, \dot{y}_k^{tc}, \ddot{y}_k^{tc})^T$ (hereafter, the subscript k will be omitted for simple notation). Estimated position and velocity of the center of a target group is used for standoff tracking guidance, which will be explained in the following section.

III. MULTITARGET TRACKING BY A UAV

A. LVFG with Variable Standoff Distance

This study applied a Lyapunov vector field guidance (LVFG) for standoff group tracking, which was initially proposed by Lawrence [39] and further developed by Frew et al. [7, 40]. The LVFG uses the vector field function:

$$V_l(x, y) = \left(r^2 - r_d^2\right)^2 \tag{12}$$

and the following desired velocity $[\dot{x}_d, \dot{y}_d]^T$:

$$\begin{bmatrix} \dot{x}_d \\ \dot{y}_d \end{bmatrix} = \frac{-v_d}{r\left(r^2 + r_d^2\right)} \begin{bmatrix} \delta x \left(r^2 - r_d^2\right) + \delta y (2 r r_d) \\ \delta y \left(r^2 - r_d^2\right) - \delta x (2 r r_d) \end{bmatrix} \tag{13}$$

or, in polar coordinates:

$$\begin{bmatrix} \dot{r} \\ r\dot{\theta} \end{bmatrix} = \frac{v_d}{r^2 + r_d^2} \begin{bmatrix} -\left(r^2 - r_d^2\right) \\ 2 r r_d \end{bmatrix} \tag{14}$$

where $\delta x = x - x^{tc}$, $\delta y = y - y^{tc}$, and $r = \sqrt{\delta x^2 + \delta y^2}$ is the distance of the UAV from the group center. Herein (x^{tc}, y^{tc}) is the center position of a target group estimated from the tracking filter as shown in Fig. 4, and v_d is the desired UAV speed. Note that the vector field is not defined at $r = 0$; r_d is a desired standoff distance from the UAV to the center of a target group, which can be computed

considering the FOV α_f of the UAV as:

$$r_d = \frac{d_{max} + d_m}{\sin\left(\frac{\alpha_f - \varepsilon_m}{2}\right)} \tag{15}$$

where $d_{\max}$ is the distance between the group center and the target furthest from the center in the group, $d_m > 0$ is a distance margin for $d_{\max}$, and $\varepsilon_m > 0$ is an angle margin for the FOV of the UAV. Compared to the single target tracking, where the target is located in the center of sensor view, the effect of uncertainty or estimation error of target information becomes more crucial to keep all the targets in view of UAVs for the group tracking. Thus, this study exploits the Mahalanobis distance concept [41, 42] to account for estimation error with relative uncertainties of the group center as:

$$d_m = \left[\mathbf{z}^{tc} - \widehat{\mathbf{z}}^{tc}\right]^T \left[P^{pos}_{k|k-1}\right]^{-1} \left[\mathbf{z}^{tc} - \widehat{\mathbf{z}}^{tc}\right] \tag{16}$$

where $\widehat{\mathbf{z}}^{tc} = H\mathbf{x}^{tc}$ is the predicted target center position, and $P^{pos}_{k|k-1}$ is the position submatrix of the prediction covariance $P_{k|k-1}$. By using the aforementioned standoff distance r_d, the UAV can keep all the targets in the group within its FOV as shown in Fig. 4. Note that a data association problem assigning which sensor measurement is from which target is not considered in this paper. However, since the proposed tracking guidance algorithm relies on the Kalman filter for tracking each target separately, it could be sensitive to false association. When multiple targets are densely positioned within a small area, the desired standoff distance can be determined more conservatively with a larger value to compensate for the error from false association and make sure all targets are within the FOV. This aspect remains as future work.

B. Convergence of the Vector Field to the Standoff Orbit

Since standoff distance r_d varies according to the movement of the individual target in the group, the convergence of the vector field to the variable loiter circle (i.e., standoff orbit) is given as the following lemma.

LEMMA 3.1 *If the threshold* $\xi_{th} = (r\dot{r} - r_d\dot{r}_d)\text{sgn}(r_d - r) \geq 0$*, then the vector field as well as the UAV position is globally stable to the loiter circle of distance* r_d *and its rate* $\dot{r}_d$.

PROOF The proof will be represented with two cases depending on the radial distance of the vehicle.

Case 1 $r < r_d$ (the UAV is inside the standoff orbit).

In this case, $\text{sgn}(r_d - r) > 0$ and $\dot{r} > 0$ from (14), where the $\text{sgn}(x)$ represents:

$$\text{sgn}(x) = \begin{cases} 1, & \text{if} \quad x > 0 \\ 0, & \text{if} \quad x = 0 \\ -1, & \text{if} \quad x < 0 \end{cases} \tag{17}$$

Let us consider the vector field function $V_l(x, y) = (r^2 - r_d^2)^2$ as defined in (12) to check the convergence of r to r_d. This vector field produces a time rate of change of V_l:

$$\begin{aligned} \dot{V}_l(x, y) &= 4\left(r^2 - r_d^2\right)(r\dot{r} - r_d\dot{r}_d) \\ &= -\frac{4v_d r\left(r^2 - r_d^2\right)^2}{\left(r^2 + r_d^2\right)} - 4r_d\left(r^2 - r_d^2\right)\dot{r}_d \end{aligned} \tag{18}$$

If $\xi_{th} = (r\dot{r} - r_d\dot{r}_d)\text{sgn}(r_d - r) \geq 0$, then the fact that $(r\dot{r} - r_d\dot{r}_d)$ is equal or greater than zero (or equivalently, $\dot{r} \geq \frac{r_d}{r}\dot{r}_d$) makes $\dot{V}_l \leq 0$. Thus, r converges to the largest invariant set $r = r_d$, satisfying $\dot{V}_r = 0$ by LaSalles's invariance principle [43], except $r = 0$, which makes the vector field globally stable to the loiter circle. Since the UAV speed is set to track the constant vector field speed, the vehicle speed converges to the vector field. Moreover, since the vector field is globally stable to the standoff orbit, so is the UAV position.

Case 2 $r \geq r_d$ (the UAV is outside the standoff orbit).

In this case, $\text{sgn}(r_d - r) \leq 0$ and $\dot{r} \leq 0$ from (14). Using the same vector field function as above, it can be easily shown that if $\xi_{th} \geq 0$ (or equivalently, $\dot{r} \leq \frac{r_d}{r}\dot{r}_d$), then $\dot{V}_l \leq 0$. Thus, r converges to the largest invariant set $r = r_d$ from the outside the loiter circle.

REMARK 3.1 *The proof of Lemma 3.1 implies that if the sign of* $\dot{r}_d$ *is different from that of* $\dot{r}$*, satisfying* $\xi_{th} \geq 0$ *in both cases, then the vector field always converges to the loiter circle.*

For $\xi_{th} < 0$, since the vector field is not guaranteed to converge to the loiter circle from Lemma 3.1, and the following holds:

$$\begin{aligned} 0 < \dot{r} < \frac{r_d}{r}\dot{r}_d, \quad & \text{if } r < r_d \\ 0 \geq \dot{r} \geq \frac{r_d}{r}\dot{r}_d, \quad & \text{otherwise} \end{aligned} \tag{19}$$

this study proposes two active measures in order to guarantee the convergence (or at least to improve the current convergence speed) of the vector field to the loiter circle by increasing $|\dot{r}|$ such that $|\dot{r}| \geq |\frac{r_d}{r}\dot{r}_d|$. The first one is done by introducing k_l in the radial equation in (14) to adjust the convergence of the vector field as:

$$\dot{r}_{new} = -\frac{v_d}{k_l}\frac{r^2 - r_d^2}{r^2 + r_d^2} \tag{20}$$

where $0 < k_l \leq 1$ is a positive constant. By doing this, a rate of change of V_l in (18) also becomes faster as:

$$\dot{V}_l(x, y) = -\frac{4v_d r\left(r^2 - r_d^2\right)^2}{k_l\left(r^2 + r_d^2\right)} - 4r_d\left(r^2 - r_d^2\right)\dot{r}_d \tag{21}$$

The second measure is to use a virtual standoff distance $r_{d,vir}$ in proportion to $\dot{r}_d$ as:

$$r_{d,vir} = r_d + k_{\dot{r}_d}\dot{r}_d \tag{22}$$

where $k_{\dot{r}_d}$ is a positive control gain. The basic idea of this is to exploit the approximated future standoff distance using the current change rate of r_d, rather than chasing the loiter circle behind it. It can be easily shown that substituting $r_{d,vir}$ from (22) into r_d of (20) increases $|\dot{r}|$ for the UAV inside as well as outside the loiter circle. However, note that these two strategies do not guarantee the convergence of the vector field all the time, especially when r_d or $\dot{r}_d$ is big due to dispersion of the targets or a high-speed vehicle in the target group. This leads to a condition for discarding a target from the group, which will be discussed in section IVB.

C. Vector Field Guidance Command

The desired heading can be decided using the desired velocity components in (13) as:

$$\psi_d = \tan^{-1}\frac{\dot{y}_d}{\dot{x}_d} \tag{23}$$

where $\tan^{-1}$ is to be executed as a four-quadrant inverse tangent in practice. The guidance command u_ω for turn rate is selected as the sum of proportional feedback and feedforward terms by differentiating (23) as:

$$u_\omega = -k_\omega(\psi - \psi_d) + \dot{\psi}_d \tag{24}$$

where

$$\dot{\psi}_d = 4v_d\frac{r_d r^2}{\left(r^2 + r_d^2\right)^2} - \frac{2r\dot{r}_d}{r^2 + r_d^2} \tag{25}$$

$\dot{\psi}_d$ can be obtained by differentiating (23). As r approaches r_d, the left term of (25) increases monotonically, and magnitude of the right term also increases. Then, the guidance vector field will be feasible as long as the loiter circle pattern itself is feasible considering variable $\dot{r}_d$, which satisfies the following when $r = r_d$:

$$\dot{\psi}_d = \frac{v_d}{r_d} - \frac{\dot{r}_d}{r_d} < \omega_{max} \tag{26}$$

Using (26), the feasible standoff distance can be determined as:

$$r_d \geq \frac{v_d}{\omega_{max}} - \frac{\dot{r}_d}{\omega_{max}} = r_{d,min} \tag{27}$$

Therefore, $r_{d,min}$ can be determined by both the maximum speed of a ground vehicle, which determines $\dot{r}_d$, and the UAV kinematic constraints ω_{max}. Note that for the guidance command to be feasible (i.e., within ω_{max}), the gain k_ω and standoff distance r_d need to be carefully determined.

D. Taking Target Group Velocity into Account

Since the velocity of the center of each group can be estimated as explained in section IIC, the guidance vector can be adjusted in order to take target velocity into account. Let us define the following relation between the new desired velocity of the UAV $[\dot{x}_{dn}, \dot{y}_{dn}]^T$ and the velocity of the target group center $[\dot{x}^{tc}, \dot{y}^{tc}]$ using a scale factor α_s and the desired x and y velocity components derived in (13) [7].

$$\begin{bmatrix}\dot{x}_{dn}\\ \dot{y}_{dn}\end{bmatrix} = \begin{bmatrix}\dot{x}^{tc} + \alpha_s\dot{x}_d\\ \dot{y}^{tc} + \alpha_s\dot{y}_d\end{bmatrix} \tag{28}$$

The condition such that the UAV flies with the desired speed v_d can be expressed by taking the norm of (28) as:

$$\begin{aligned}&\left(\dot{x}_d^2 + \dot{y}_d^2\right)\alpha_s^2 + 2\left(\dot{x}_d\dot{x}^{tc} + \dot{y}_d\dot{y}^{tc}\right)\alpha_s\\ &\quad + \left(\dot{x}^{tc}\right)^2 + \left(\dot{y}^{tc}\right)^2 - v_d^2 = 0\end{aligned} \tag{29}$$

This equation has one positive real solution for α_s only if the desired speed of the UAV is larger than the target speed. Substituting this solution into (28) yields the modified desired guidance vector of the UAV.

IV. COORDINATED MULTITARGET TRACKING BY MULTIPLE UAVS

This section proposes a multitarget group surveillance strategy by cooperating multiple UAVs with benefits such as better estimation accuracy with sensor/data fusion and more robust tracking performance. Since multitarget tracking using multiple UAVs is typically NP-hard both in the number of sensing agents and targets [27], this study uses a two-step approach: 1) target clustering/resource allocation; and 2) cooperative standoff group tracking with local replanning.

A. Target Clustering and Resource Allocation

Since this study uses a standoff tracking concept in which UAVs are continuously orbiting around moving targets, one of the suboptimal approaches to partition the targets would be treating geographically close targets as the same target group. This is done by a K-means clustering algorithm to group objects based on attributes into a predefined K number of groups [44]. The grouping is done by minimizing the sum of squares of distances between data and the corresponding cluster centroid as Algorithm 1, where the optimization objective J is in the

ALGORITHM 1 K-means algorithm to cluster multiple targets.

Input K (number of clusters) and target position data $\{x_{pos}^1, \cdots, x_{pos}^m\}$
1: Randomly initialize K cluster centroids $\mu_1, \mu_2, \ldots, \mu_k \in \mathbb{R}^2$
2: while $\Delta J > \epsilon$ $\{J :=$ optimization objective [(30)]$\}$ do
3: for $i = 1$ to m do
4: Compute $c^{(i)} :=$ index (from 1 to K) of cluster centroid closest to $\mathbf{x}_{pos}^i$
5: end for
6: for $k = 1$ to K do
7: Compute $\mu_k :=$ average (mean) of target positions assigned to cluster k
8: end for
9: end while

form:

$$J\left(c^{(1)},\ldots,c^{(m)},\mu_1,\mu_2,\ldots,\mu_K\right)=\frac{1}{m}\sum_{i=1}^{m}\left\|x_{pos}^{i}-\mu_{c^{(i)}}\right\| \tag{30}$$

where c^i is the index of clusters closest to the target point x_{pos}^i, and $\mu_{c^{(i)}}$ is the centroid position of cluster c^i, equivalently, the mean of target positions assigned to that cluster. This study considers the situation where either one or two UAVs are engaging the same target group; thus the number of clusters is determined by the number of UAVs, N_u as $N_{tg}=\text{round}\left(\frac{N_u}{2}\right)$, where round$(\cdot)$ represents rounding the inside element to the nearest integer.

After clustering, UAVs need to be assigned to the corresponding target group. The optimal assignment approach is used as the one that gathers the most information about targets using a Fisher information matrix (FIM). The FIM describes the amount of information a set of measurements contains about the state variable in terms of sensitivity of the estimation process [21]. Thus, maximizing the FIM is more likely to improve the estimation performance and to reduce uncertainty as used in guidance law design [45, 46], trajectory optimization [47, 48], and observability criteria analysis [49] using a bearing-only sensor. In this regard, initial assignment of UAVs that yields large values of some measure of the FIM is expected to yield better estimation performance compared to those that give lower values. The details of the FIM can be found in [21, 50]. Assuming that prior information is always ignored, the FIM for multiple UAVs to a single target is given as:

$$\begin{aligned}I^{FIM}&=\sum_{i=1}^{N_u}H_i^T R_i^{-1}H_i\\&=\sum_{i=1}^{N_u}\begin{bmatrix}\frac{\cos^2\theta_i}{\sigma_r^2}+\frac{\sin^2\theta_i}{r_i^2\sigma_\theta^2} & \frac{\cos\theta_i\sin\theta_i}{\sigma_r^2}-\frac{\cos\theta_i\sin\theta_i}{r_i^2\sigma_\theta^2}\\ \frac{\cos\theta_i\sin\theta_i}{\sigma_r^2}-\frac{\cos\theta_i\sin\theta_i}{r_i^2\sigma_\theta^2} & \frac{\sin^2\theta_i}{\sigma_r^2}+\frac{\cos^2\theta_i}{r_i^2\sigma_\theta^2}\end{bmatrix}\end{aligned} \tag{31}$$

where θ_i represents the bearing angle of ith UAV to the target. The determinant $\eta_D=\det(I^{FIM})$ is used to measure the size of the FIM. Then, the assignment solution to maximize the FIM can be obtained by solving the following formulation:

$$\max J=\det\left(\sum_{i=1}^{N_s}\sum_{j=1}^{N_{tg}}I_{ij}^{FIM}x_{ij}\right) \tag{32}$$

$$\sum_{j=1}^{N_{tg}}x_{ij}\le 1,\ x_{ij}\in\{0,1\},\quad \text{for}\, i=1,\ldots,N_s \tag{33}$$

where $N_s=2^{N_u}-1$ is the number of possible combinations of N_u UAVs to observe the target group, and I_{ij}^{FIM} represents the FIM of ith UAV combination assigned to jth target group. Equation (33) represents that one target group is assigned to one UAV combination at most. Note that this optimization process is performed only once at the initial stage.

B. Online Local Replanning

Once initial assignment of UAVs to target groups is done, online local replanning is followed, either by handing over targets between groups or discarding a target out of the group according to sensing range or the convergence of the vector field while UAVs are persistently following corresponding groups.

1) *Target Handoff*: By running a K-means clustering algorithm in a recursive manner, a target handoff event between groups can be done inherently, since clustering itself can regroup targets according to their proximity to the target group and UAVs. To avoid frequent change of the group for a target on the boundary between two (passing/receiving) groups, as well as to make sure that the target passed to the receiving group is inside the FOV of UAVs of that group, handoff occurs for a certain period of time T_{hd}:

$$T_{hd}\ge\left[\frac{|r-r_d|}{|\dot{r}_{new}-\frac{r_d}{r}\dot{r}_d|}\right]_{t=t_{hd}^i} \tag{34}$$

where t_{hd}^i represents the time when the target is first requested for the handoff by the clustering algorithm. For T_{hd}, the handoff target will be included in both passing and receiving groups. Until UAVs for the receiving group reach the desired standoff orbit, keeping the handoff target in their FOV, the UAV for the passing group sends the position of the handoff target to the receiving group.

2) *Target Discard*: If the standoff distance for the group tracking becomes larger than the sensing range (i.e., $r_d>r_{d,max}$), or the radial velocity difference between the vector field and desired standoff orbit is larger than a certain value (i.e., $\xi_{th}<-\xi_d$ from Lemma 3.1), the target furthest from the center in the group is removed from the group.

C. Sensitivity Analysis to Orbit Coordination

In case that a pair of UAVs are involved for the same target group, the angular separation between UAVs is additionally performed by controlling the speed of UAVs in order to obtain more accurate target information and to avoid collision between them as explained in [7]:

$$u_v=\pm k_v(\gamma-\theta_d)r_d+v_d \tag{35}$$

where k_v is a control gain, θ_i is the azimuth angle of the ith UAV relative to the group center, $\gamma=\theta_2-\theta_1$ is the angular phase separation of UAVs, and θ_d is a desired phase difference between the UAVs. Different approaches to this angular separation can be applied, such as controlling the orbit radius instead of the speed [15, 19] and using a decentralized approach for more than two UAVs [20, 35]. During the target handoff process, physical collision between UAVs in different groups could be avoided by operating them in different altitudes for each target group or using a local collision avoidance algorithm [51].

The desired phase difference θ_d can be determined differently depending on the objective of the mission, such as estimation accuracy or visibility of an adversarial target. This study adopts the strategy that maximizes

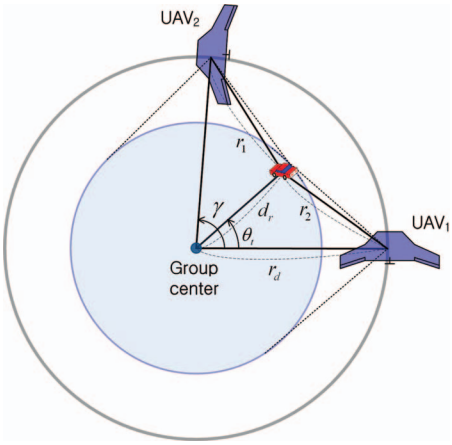

Fig. 5. Geometric relation between UAVs and ground target.

information (or equivalently, provides the best estimation accuracy) in the current measurements without considering previous information using the FIM as used in the previous section. The determinant of the FIM from two UAVs for the same single target can be given using (31) and trigonometric identities as:

$$\eta_{D,pair} = \det\left(\sum_{i=1}^{2} H_i^T R_i^{-1} H_i\right) = \frac{1+\cos^2\gamma}{\sigma_r^2\sigma_\theta^2}\left(\frac{1}{r_1^2}+\frac{1}{r_2^2}\right)+\left(\frac{\sin^2\gamma}{\sigma_r^4}+\frac{\sin^2\gamma}{\sigma_\theta^4 r_1^2 r_2^2}\right) \tag{36}$$

For single target tracking, the optimal value of γ that maximizes η_D can be analytically obtained from (36). It can be easily shown that the value is $\pi/2$ when two UAVs have the same distance to the target (i.e., $r_1 = r_2 = r_d$ on the same standoff orbit) to maximize the information UAVs can obtain from the target. However, in this study, since the targets are dispersed around the group center, it is difficult for a pair of UAVs loitering around the same target group to determine one specific optimal γ. To check a tendency of η_D depending on target position specified with the range $0 \le d_r \le 180$ m and angle $0 \le \theta_t < 360^\circ$ from the group center, numerical analysis is performed for different angular separation γ_{sep} with fixed $r_d = 400$ m as illustrated in Fig. 7. For the analysis, the standard deviation of measurement noise is generalized with $\sigma_{scale} = \frac{r_d\sigma_q}{\sigma_r}$ such that the small scale represents sensor characteristics close to bearing-only, and the large value represents pure ranging.

First, Fig. 5 shows the example of $\eta_{D,norm}$ (scaled by $\eta_{D,0}$ with $d_r = 0$, $\theta_t = 0^\circ$, and $\gamma_{sep} = 90^\circ$) for specific angular separations ($\gamma_{sep} = 0^\circ, 90^\circ, 180^\circ$) for $\sigma_{scale} = 1$. This shows that η_D, the determinant of the FIM, is substantially subject to the distance of the target from UAVs, which is determined by d_r and θ_t. For instance, in Fig. 5a, when UAVs and the target are closest (or, in turn, θ_t is zero and d_r is the maximum), $\eta_{D,norm}$ has the highest value, and it decreases as the target gets further away from UAVs until reaching $\theta_t = 180^\circ$, which shows the lowest value. After this point, as the target gets closer to UAVs again, $\eta_{D,norm}$ tends to increase, resulting in a symmetrical evolution with respect to $\theta_t = 180^\circ$. Depending on the location of UAVs (or separation angle γ_{sep}), $\eta_{D,norm}$ shows a different but similar periodic evolution as shown in Figs. 5b and 5c. Fig. 6 shows $\eta_{D,norm}$ (averaged for all θ_t) for different σ_{scale} with respect to the target distance d_r and angular separation γ_{sep}. For $\sigma_{scale} = 0.01$ in Fig. 6a, both the optimality criterion and the optimal value of γ_{sep} change as a function of the range d_r, since this configuration is close to a bearing-only measurement as explained above. For $\sigma_{scale} = 100$ (or, pure ranging), the optimality criterion changes as γ_{sep} changes, and the optimal value remains around $\pi/2$ independent of d_r. Last, in case of a sensor with $\sigma_{scale} = 1$ (i.e., range and bearing sensor such as a GMTI), $\eta_{D,norm}$ is only a function of range for small d_r (<100 m); however, angular separation has some effect on it as d_r gets larger. The implication with which Fig. 6 shows that the optimal separation angle γ between UAVs varies depending on the distance (d_r) of the target from the group center and sensor characteristics; however, the optimal angle still stays around 90°, which is similar to the single target tracking case. Thus, 90° is used as the separation angle between UAVs on the same standoff orbit in the following numerical simulation section. In addition, although an online algorithm to determine the optimal γ_{sep} could be developed for better group tracking performance based on this analysis, it remains as future work.

V. NUMERICAL SIMULATIONS

This section carries out numerical simulations using the proposed standoff group tracking algorithm for moving ground targets using multiple UAVs to show the feasibility and benefits of the proposed approach. The true target trajectories (randomly moving by target model as in section IIB) are used to generate GMTI measurements at 2 Hz mixing with white Gaussian noise. The parameters used for the simulation are shown in Table I.

First, the localization and tracking guidance performance for a single group of four randomly moving targets using either a single or two UAVs are shown in Table II. For this, Monte Carlo simulations with 200 independent runs (for which the sample run is shown in Fig. 8) are performed, and then the results are averaged. Localization error in position and velocity of targets using multiple UAVs is less than that of a single UAV case with the help of sensor fusion using the decentralized EIF. The MVSD-LVFG (modified LVFG algorithm with a variable standoff distance [VSD] and two active measures as explained in section IIIB) shows much better performance than that of the VSD-LVFG in terms of standoff distance tracking and phase angle keeping. In line with this, the mean value of the maximum LOS angle from the UAV to the targets is the lowest when using the MVSD-LVFG as a

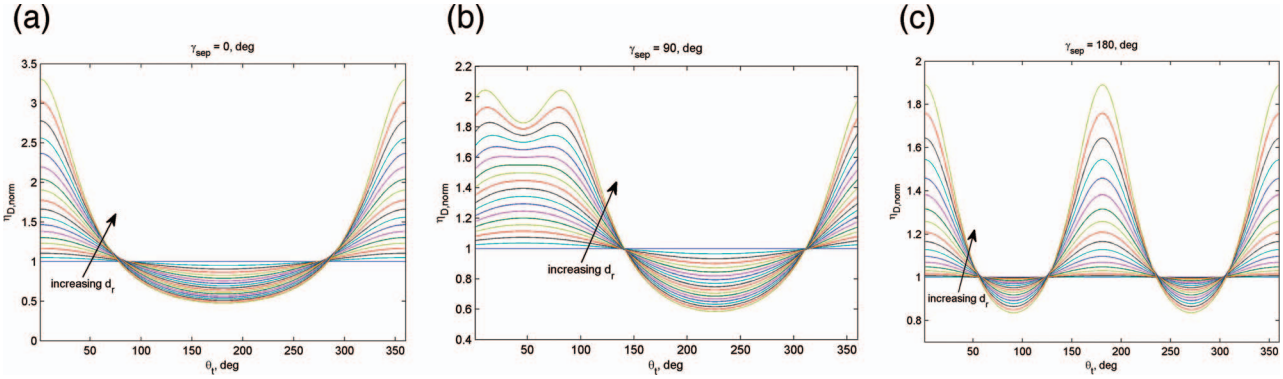

Fig. 6. Nondimensional η_D with respect to (w.r.t) target distance from group center (d_r) and specific angular separations ($\gamma_{sep} = 0^\circ, 90^\circ, 180^\circ$) for $\sigma_{scale} = 1$.

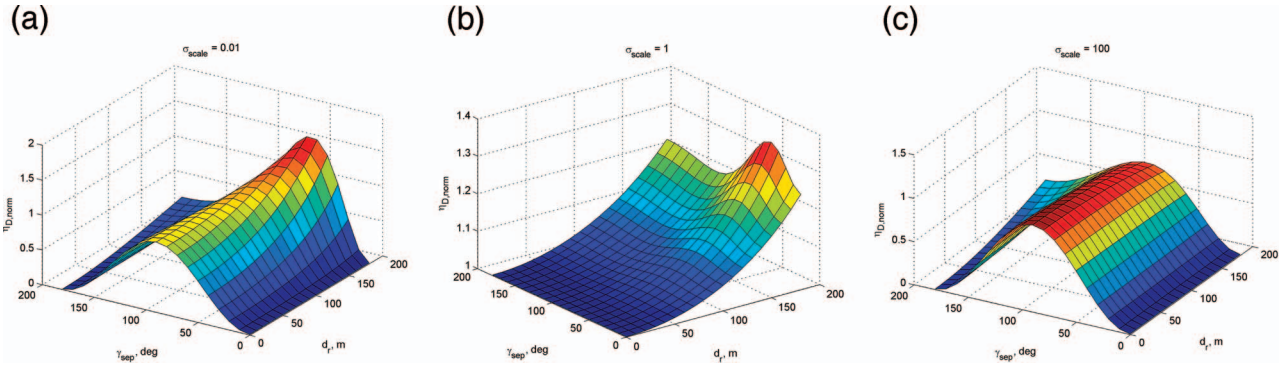

Fig. 7. Nondimensional η_D (average for $0 \leq \theta_t < 360^\circ$) w.r.t. target distance from group center (d_r) and angular separation (γ_{sep}) for different values of scaled noise standard deviation.

TABLE I
Simulation Parameters

Parameter	Value	Unit
T_s	0.5	s
α	0.1	N/A
$(\alpha_f, \varepsilon_m)$	(70,10)	deg
$(\sigma_r, \sigma_\theta)$	(10, 3)	(m, deg)
θ_d	90	deg
v_0	40	m/s
$(r_{d,min}, r_{d,max})$	(250,700)	m
Δv_{max}	15	m/s
ω_{max}	0.3	rad/s
τ_v,τ_ω	1/3	s
$(k_v, k_w, k_l, k_{\dot{r}_d})$	(0.5,2,0.2,3)	N/A

TABLE II
Tracking Performance for a Group of Four Targets (Averaged over 200 Monte Carlo Simulations)

	Single UAV	Multiple UAVs	
Mean Error	VSD-LVFG[a]	VSD-LVFG	MVSD-LVFG[b]
Position (m)	9.5227	6.8615	6.8570
Velocity (m/s)	1.6252	1.2887	1.2768
Standoff distance (m)	31.5984	29.8649	9.1261
Phase keeping (deg)	–	2.3173	1.6205
Line-of-sight (deg)	15.6864	15.4000	14.5131

[a]LVFG with a variable standoff distance (VSD).
[b]Modified VSD-LVFG.

result of precise standoff orbit tracking; this means all targets are more likely to be within the UAV sensor FOV.

Fig. 9 shows the absolute trajectories of seven ground target (six randomly moving and one maneuvering) with four UAVs using the proposed standoff tracking framework. First, targets are clustered into two groups, and UAVs are assigned to the appropriate group using the proposed assignment algorithm as shown in Fig. 9a. Note that data association regarding which measurement comes from which target is assumed to be solved as mentioned in section II in this study. However, since our approach to track multiple targets is to exploit the center of the group and furthest target information from the center only, even some false data association at the beginning in a cluttered situation as shown in Fig. 9a would not affect the guidance performance in terms of keeping all targets in the standoff orbit. At around 35 s since the target handoff event was triggered, the target (moving toward the northeast direction) is included in both target groups until UAVs of the receiving group (group 2) reach the desired standoff orbit for T_{hd} seconds as shown in Fig. 9b and Fig. 10a. Fig. 9c shows the situation after the target handoff (from group 1 to group 2) process is finished. As targets in the group get dispersed widely, the furthest target from the center is removed from the group depending on the sensing range or convergent limit as introduced in section IVB. The Mahalanobis distance in Fig. 10c is used to account for estimation error of the group center position

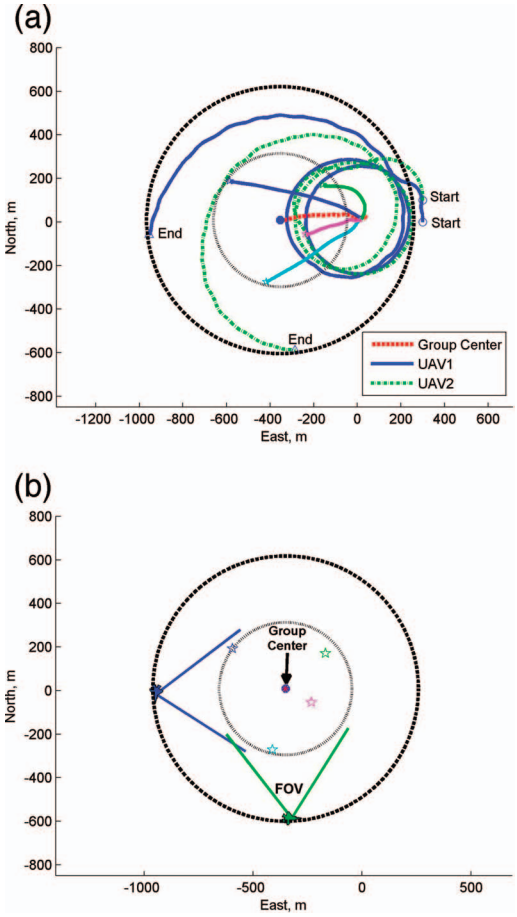

Fig. 8. Absolute trajectories of standoff tracking of four ground targets with two UAVs.

when the group center changes abruptly due to target handoff or discard, and it shows the same tendency as center position estimation error (i.e., $|x^{tc}_{true} - x^{tc}|$), as shown in Fig. 10d. Figures 9 and 10 show successful cooperative standoff group tracking results in terms of standoff distance error and desired angular separation while placing all targets of interest inside the FOV of the UAV at all times in a dynamic environment.

Fig. 11 represents the LOS angle history between UAVs and the furthest target from the target group center using the same scenario as above but with either 1) basic standoff tracking guidance or 2) the two active guidance measures explained in section III and the target handoff time T_{hd}. In this figure, when the LOS angle to the furthest target (or the maximum LOS) is less than half of the FOV, all the targets can be regarded to be inside the FOV of the UAV. In the basic guidance case shown in Fig. 11a, the maximum LOS angle is often higher or close to the FOV limit (represented as black dashed line) as a desired loiter circle expands/contracts rather quickly. In addition, due to the frequent group change of the target on the boundary between two groups during target handoff, the maximum LOS angle gets significantly higher than the FOV limit for around 35 to 40 s. On the other hand, in the latter case (Fig. 11b), the maximum LOS angle is always less than half of the FOV since the proposed active measures enhance the convergence property of the UAV to the loiter circle and T_{hd} prevents the abrupt change of the target group while ensuring the handoff target can be inside the FOV of UAVs in the receiving group. Movie clips for standoff tracking guidance simulations, including the two cases presented here, can be downloaded at https://dl.dropboxusercontent.com/u/17047357/MultiTracking.zip.

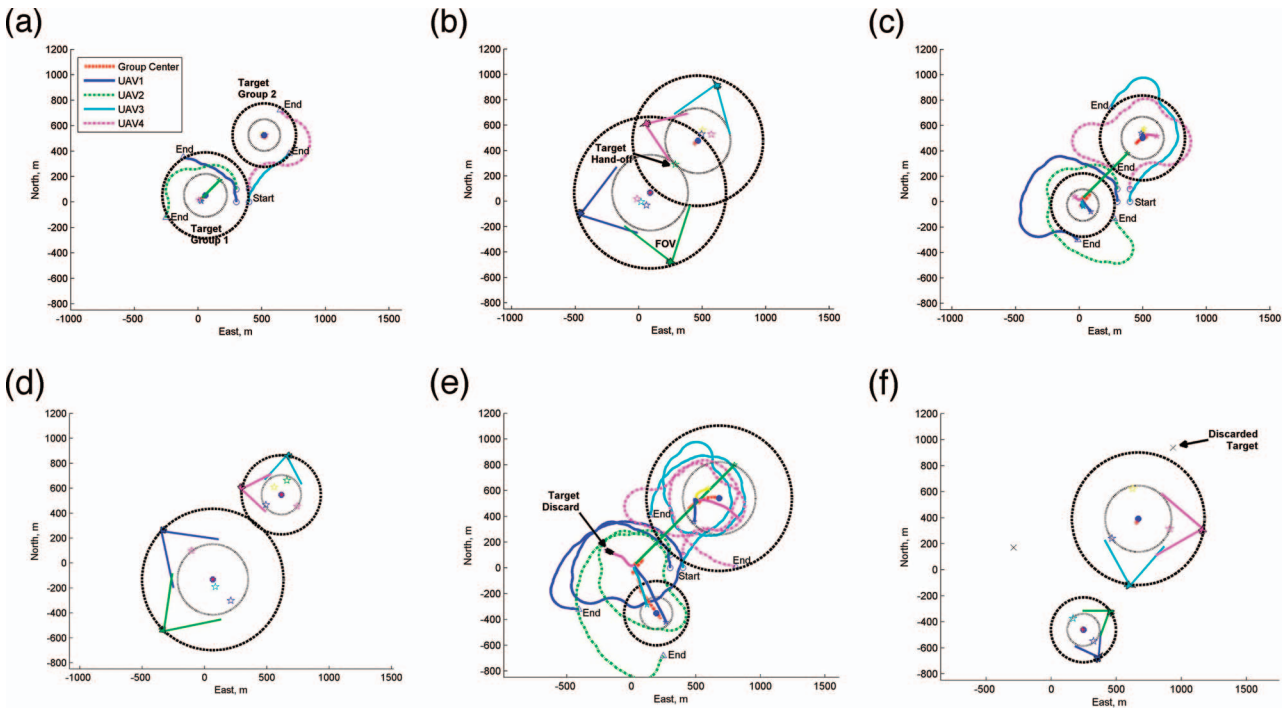

Fig. 9. Absolute trajectories of standoff tracking of seven ground targets (six randomly moving and one maneuvering) with four UAVs.

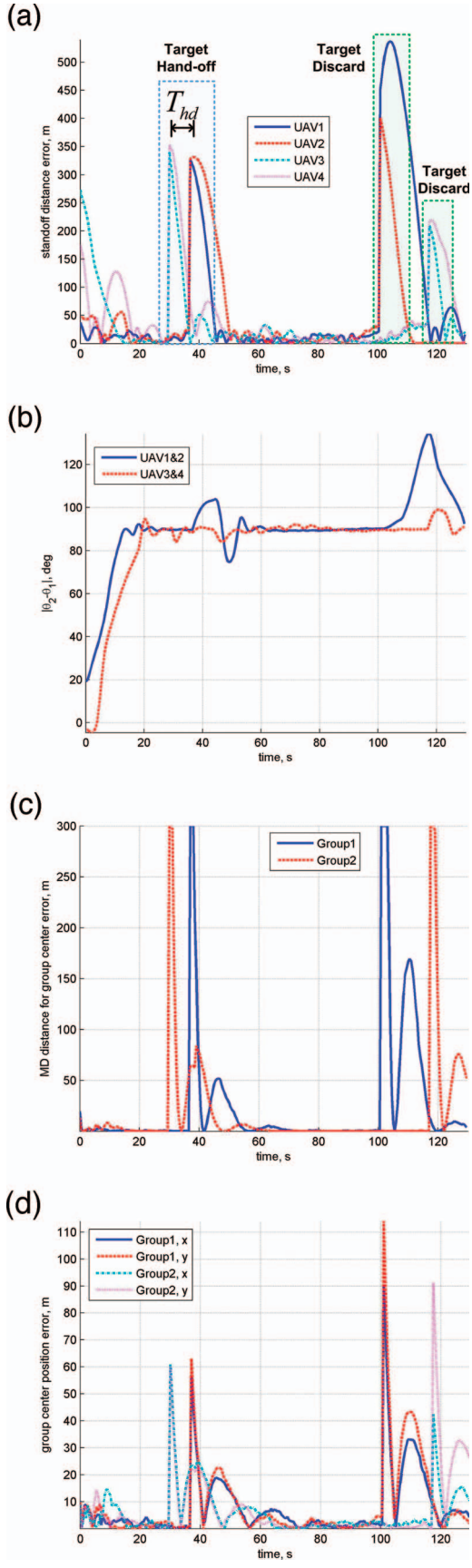

Fig. 10. Standoff tracking simulation results of seven ground targets (six randomly moving and one maneuvering) with four UAVs.

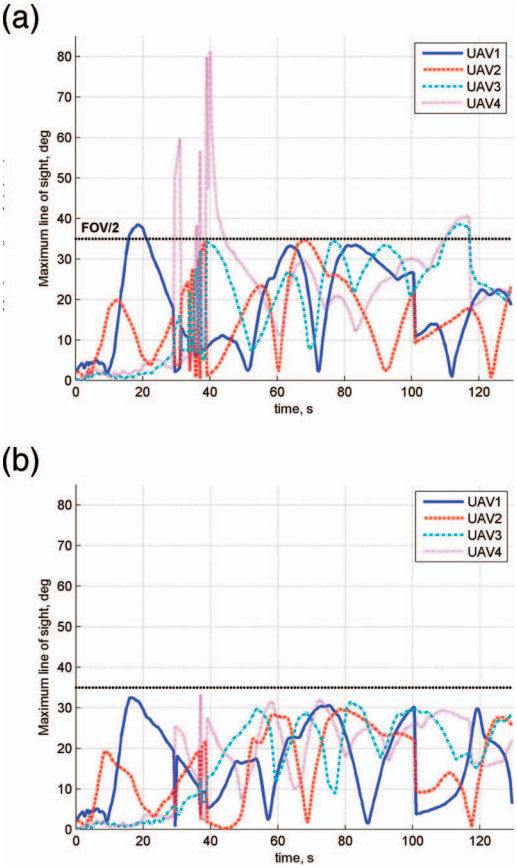

Fig. 11. Line-of-sight angle between UAVs and furthest target from center of corresponding target group.

VI. CONCLUSIONS AND FUTURE WORK

This paper has presented the coordinated standoff tracking of moving target groups using multiple UAVs. Based on the vector field guidance approach, an active sensing/guidance algorithm was developed to maximize information of the targets and keep all targets inside the view of multiple UAVs considering physical and sensing constraints. For multiple group target surveillance by multiple UAVs, a two-phase approach was proposed consisting of target clustering/assignment and cooperative standoff tracking with online local replanning, including target handoff and discard from the group. Localization sensitivity to the group of targets was also investigated for different angular separations between UAVs and sensing configurations as a basis of future optimal separation schemes. Numerical simulation showed successful standoff group tracking as well as local replanning while keeping all targets of interest within the FOV of the UAV at all times in a dynamic environment. Since this study is in the phase of the initial proof of concept, various implementation issues will be tackled as future work, such as the effect of imperfect communication between UAVs, and measurement data association in conjunction with group clustering and angular spacing strategies in consideration of LOS blockage by obstacles in an urban environment. Redesign of the proposed algorithm for

systems that can hover will be considered as well, because this could greatly improve the performance without constraints of fixed-wing UAVs such as the minimum speed and the maximum turn rate. In addition, inclusion of no-fly zones and other restrictions due to cross winds in an urban environment will be considered in the future work.

REFERENCES

[1] Girard, A. R., Howell, A. S., and Hedrick, J. K.
Border patrol and surveillance missions using multiple unmanned air vehicles.
In *43rd IEEE Conference on Decision and Control*, Bahamas, Dec. 2004.

[2] Kingston, D., Beard, R. W., and Holt, R. S.
Decentralized perimeter surveillance using a team of UAVs.
IEEE Transactions on Robotics, **24**, 6 (2008), 1394–1404.

[3] Kontitsis, M., Valavanis, K. P., and Tsourveloudis, N. A
UAV vision system for airborne surveillance.
In *IEEE International Conference on Robotics and Automation*, New Orleans, LA, April–May 2004.

[4] Pitre, R. R., Li, X. R., and Delbalzo, R.
UAV route planning for joint search and track mission—an informative-value approach.
IEEE Transactions on Aerospace and Electronic Systems, **48**, 3 (2012), 2551–2565.

[5] Puri, A.
A survey of unmanned aerial vehicles (UAV) for traffic surveillance.
Department of Computer Science and Engineering, University of South Florida, Tampa, FL, Technical Rep., 2004.

[6] Carapezza, E. M., and Law, D. B.
Sensors, C3I, information, and training technologies for law enforcement.
In *Proceedings SPIE*, Boston, MA, Jan. 1999.

[7] Frew, E. W., Lawrence, D. A., and Morris, S.
Coordinated standoff tracking of moving targets using Lyapunov guidance vector fields.
Journal of Guidance, Control, and Dynamics, **31**, 2 (2008), 290–306.

[8] Chen, H.
UAV path planning with tangent-plus-Lyapunov vector field guidance and obstacle avoidance.
IEEE Transactions on Aerospace and Electronic Systems, **49**, 2 (2013), 840–856.

[9] Lim, S., Kim, Y., Lee, D., and Bang, H.
Standoff target tracking using a vector field for multiple unmanned aircrafts.
Journal of Intelligent and Robotic System, **69**, 1–4 (2013), 347–360.

[10] Zhu, S., and Wang, D.
Adversarial ground target tracking using UAVs with input constraints.
Journal of Intelligent and Robotic System, **65**, 14 (2012), 521–532.

[11] Zhu, S., Wang, D., and Low, C. B.
Ground target tracking using UAV with input constraints.
Journal of Intelligent and Robotic System, **69**, 14 (2013), 417–429.

[12] Shames, I., Dasgupta, S., Fidan, B., and Anderson, B. D. O.
Circumnavigation using distance measurements under slow drift.
IEEE Transactions on Automatic Control, **57**, 4 (2012), 889–903.

[13] Deghat, M., Shames, I., Anderson, B. D. O., and Yu, C.
Target localization and circumnavigation using bearing measurements in 2D.
In *49th IEEE Conference on Decision and Control*, Atlanta, GA, Dec. 2010.

[14] Livermore, R. A.
Optimal UAV path planning for tracking a moving ground vehicle with a gimbaled camera. Master's thesis,
U.S. Air Force Institute of Technology (USAF),
Wright-Patterson AFB, OH, 2014.

[15] Wise, R. A., and Rysdyk, R. T.
UAV coordination for autonomous target tracking.
In *AIAA Guidance, Navigation and Control Conference*, Keystone, CO, 2006.

[16] Kim, J., and Kim, Y.
Moving ground target tracking in dense obstacle areas using UAVs.
In *IFAC World Congress*, COEX, South Korea, 2008.

[17] Yoon, S., Park, S., and Kim, Y.
Circular motion guidance law for coordinated standoff tracking of a moving target.
IEEE Transactions on Aerospace and Electronic Systems, **49**, 4 (2013), 2440–2462.

[18] Kim, S., Oh, H., and Tsourdos, A.
Nonlinear model predictive coordinated standoff tracking of moving ground vehicle.
Journal of Guidance, Control and Dynamics, **36**, 2 (2013), 557–566.

[19] Kingston, D., and Beard, R.
UAV splay state configuration for moving targets in wind.
Lecture Notes in Control and Information, **369** (2007), 109–128.

[20] Summers, T. H., Akella, M. R., and Mears, M. J.
Coordinated standoff tracking of moving targets: control laws and information architectures.
Journal of Guidance, Control, and Dynamics, **32**, 1 (2009), 56–69.

[21] Frew, E. W.
Sensitivity of cooperative target geolocalization to orbit coordination.
Journal of Guidance, Control, and Dynamics, **31**, 4 (2008), 1028–1040.

[22] Oh, H., Kim, S., Tsourdos, A., and White, B. A.
Road-map assisted standoff tracking of moving ground vehicle using nonlinear model predictive control.
In *American Control Conference*, Montreal, Canada, June 2012.

[23] Oh, H., Kim, S., Shin, H. S., Tsourdos, A., and White, B. A.
Behaviour recognition of ground vehicle using airborne monitoring of UAVs.
International Journal of Systems Science, **45**, 12 (2014), 2499–2514.

[24] Kim, S., Zbikowski, R. W., Tsourdos, A., and White, B. A.
Airborne monitoring of ground traffic behaviour for hidden threat assessment.
In *13th International Conference on Information Fusion*, Edinburgh, UK, July 2010.

[25] Parker, L.
Distributed algorithms for multi-robot observation of multiple moving targets.
Autonomous Robots, **12**, 3 (2002), 231–255.

[26] Jung, B., and Sukhatme, G. S.
A region-based approach for cooperative multi-target tracking in a structured environment.
In *IEEE/RSJ International Conference on Intelligent Robots and Systems*, Lausanne, Switzerland, 2002, 2764–2769.

[27] Tang, Z., and Ozguner, U.
Motion planning for multitarget surveillance with mobile sensor agents.
IEEE Transactions on Robotics, **21**, 5 (2005), 898–908.

[28] Ousingsawat, J., and Campbell, M. E.
Optimal cooperative reconnaissance using multiple vehicles.
Journal of Guidance, Control and Dynamics, **30**, 1 (2007), 122–132.

[29] Deghat, M., Xia, L., Anderson, B. D. O., and Hong, Y.
Multi-target localization and circumnavigation by a single agent using bearing measurements.
International Journal of Robust and Nonlinear Control, 2014, to be published. doi:10.1002/rnc.3208.

[30] Lawrence, D. A., Frew, E. W., and Pisano, W. J.
Lyapunov vector fields for autonomous unmanned aircraft flight control.
Journal of Guidance, Control, and Dynamics, **31**, 5 (2008), 1220–1229.

[31] SIAS Limited. S-Paramics software, http://www.sias.com, last access Jan. 2011.

[32] Mehrotra, K., and Mahapatra, P. R.
A jerk model for tracking highly maneuvering targets.
IEEE Transactions on Aerospace and Electronic Systems, **33**, 4 (1997), 1094–1105.

[33] Koch, W., Koller, J., and Ulmke, M.
Ground target tracking and road map extraction.
ISPRS Journal of Photogrammetry and Remote Sensing, **61**, 3–4 (2006), 197–208.

[34] Mutambara, A. G. O.
Decentralized Estimation and Control for Multisensor Systems. Boca Raton, FL: CRC Press LLC, 1998.

[35] Oh, H., Kim, S., Tsourdos, A., and White, B. A.
Decentralised road-map assisted ground target tracking using a team of UAVs.
In *9th IET Data Fusion & Target Tracking*, London, UK, May 2012.

[36] Lerro, D., and Bar-Shalom, Y.
Tracking with debiased consistent converted measurements versus EKF.
IEEE Transactions on Aerospace and Electronic Systems, **29**, 3 (1993), 1015–1022.

[37] Lei, M., and Han, C.
Sequential nonlinear tracking using UKF and raw range-rate measurements.
IEEE Transactions on Aerospace and Electronic Systems, **43**, 1 (2007), 239–250.

[38] Bordonaro, S. V., Willett, P., and Bar-Shalom, Y.
Consistent linear tracker with position and range rate measurements.
In *Record of the Forty Sixth Asilomar Conference on Signals, Systems and Computers (ASILOMAR)*, Pacific Grove, CA, Nov. 2012.

[39] Lawrence, D. A.
Lyapunov vector fields for UAV flock coordination.
In *2nd AIAA Unmanned Unlimited Conference, Workshop, and Exhibit*, San Diego, CA, Sept. 2003.

[40] Morris, S., and Frew, E. W.
Cooperative tracking of moving targets by teams of autonomous unmanned air vehicles.
MLB Company, Santa Clara, CA, Technical Rep. FA955004-C-0107, 2005.

[41] Cox, I. J.
A review of statistical data association techniques for motion correspondence.
International Journal of Computer Vision, **10**, 1 (1993), 53–66.

[42] Massart, D. L., De Maesschalck, R., and Jouan-Rimbaud, D.
The Mahalanobis distance.
Chemometrics and Intelligent Laboratory Systems, **50**, 1 (2000), 1–18.

[43] Khalil, H. K.
Nonlinear Systems, 3rd ed. Upper Saddle River, NJ: Prentice Hall, 2002.

[44] Bishop, C. M.
Neural Networks for Pattern Recognition. Oxford, United Kingdom: Oxford University Press, 1995.

[45] Lee, W., Bang, H., and Leeghim, H.
A cooperative guidance law for target estimation by multiple unmanned aerial vehicles.
ImechE Part G: Journal of Aerospace Engineering, **225**, 12 (2011), 1322–1335.

[46] Passerieux, J. M., and Van Cappel, D.
Optimal observer maneuver for bearings-only tracking.
IEEE Transactions on Aerospace and Electronic Systems, **34**, 3 (1998), 777–788.

[47] Ponda, S. S., Kolacinski, R. M., and Frazzoli, E.
Trajectory optimization for target localization using small unmanned aerial vehicles.
In *AIAA Guidance, Navigation and Control Conference*, Chicago, IL, Aug. 2009.

[48] Oshman, Y., and Davidson, P.
Optimization of observer trajectories for bearing-only target localization.
IEEE Transactions on Aerospace and Electronic Systems, **35**, 3 (1999), 892–902.

[49] Woffinden, D. C., and Geller, D. K.
Observability criteria for angles-only navigation.
IEEE Transactions on Aerospace and Electronic Systems, **45**, 3 (2009), 1194–1208.

[50] Taylor, J. H.
Cramer-Rao estimation error lower bound computation for deterministic nonlinear systems.
IEEE Transactions on Automatic Control, **24**, 2 (1979), 343–344.

[51] Han, S. C., Bang, H., and Yoo, C. S.
Proportional navigation-based collision avoidance for UAVs.
International Journal of Control, Automation and Systems, **7**, 4 (2009), 553–565.

Hyondong Oh received the B.Sc. and M.Sc. degrees in aerospace engineering from Korea Advanced Institute of Science and Technology (KAIST), South Korea, in 2004 and 2010, respectively, and then he acquired a Ph.D. on autonomous surveillance and target tracking guidance using multiple UAVs from Cranfield University, United Kingdom, in 2013. He worked as a postdoctoral research associate on the European Commission FP7 Project "SWARM-ORGAN" at Nature Inspired Computing and Engineering (NICE) Group, University of Surrey, United Kingdom. He is currently a lecturer in autonomous unmanned vehicles at Loughborough University, United Kingdom.

Seungkeun Kim received a B.Sc. degree in mechanical and aerospace engineering from Seoul National University (SNU), Seoul, Korea, in 2002, and then acquired a Ph.D. from SNU in 2008. He is currently an assistant professor at the Department of Aerospace Engineering, Chungnam National University, Korea. Previously he was a research fellow and a lecturer at Cranfield University, United Kingdom, in 2008–2012. He has published book chapters, journal articles, and conference papers related to unmanned systems. His research interests cover nonlinear guidance and control, estimation, sensor and information fusion, fault diagnosis, fault tolerant control, and decision making for unmanned systems.

Hyo-Sang Shin received his B.Sc. from Pusan National University and gained an M.Sc. on flight dynamics, guidance, and control in aerospace engineering from KAIST and a Ph.D. on cooperative missile guidance from Cranfield University. He is currently a lecturer on guidance, control, and navigation systems at the Centre for Cyber-Physical Systems at Cranfield University. He has actively published book chapters, journal articles, and conference papers and has been invited for many lectures at universities, industries, and research institutes. His current research interests include decision making on multi-agent systems, improvement of multiple vehicle cooperation, coordinated heath monitoring and management, and information-driven sensing.

Antonios Tsourdos obtained an M.Eng. on electronic, control and systems engineering from the University of Sheffield (1995), an M.Sc. on systems engineering from Cardiff University (1996), and a Ph.D. on nonlinear robust missile autopilot design and analysis from Cranfield University (1999). He is a professor of control engineering with Cranfield University, appointed as the head of the Centre for Cyber-Physical Systems in 2013. Professor Tsourdos was member of Team Stellar, the winning team for the United Kingdom Ministry of Defence Grand Challenge (2008) and the Institution of Engineering and Technology Innovation Award (Category Team, 2009).